Journal of Geological Resource and Engineering 7 (2019) 113-122
doi:10.17265/2328-2193/2019.04.001

Features of the Mineral Composition of the Quaternary Sediments of the Development Areas of the Erosion Processes on the Territory of the Tunkinsk's Depression

S. I. Shtel'makh[1], L. A. Pavlova[2] and T. G. Ryashchenko[1]

1. Institute of the Earth's Crust, SB RAS, 128 Lermontov St., Irkutsk 664033, Russia

2. Institute of Geochemistry Named after A. P. Vinogradov, SB RAS, 1A Favorskiy St., Irkutsk 664033, Russia

Abstract: The article considers the some features of the Quaternary sediments mineral composition of the development areas of the erosion processes on the territory of the Tunkinsk's depression. Main objectives of our research are to determine the entering forms of Na, Mg, Al, Si, P, S, K, Ca, Ti, Cr, Mn, Fe, Zn, Cu, Zr, and Ba in the composition of the investigated sediments. The mineral composition was studied by the method of an electron probe X-ray spectral microanalysis (XRM) using wave spectrometers, and the method of X-ray diffraction analysis. The localization centers of Cr, Cu, Zn, Zr, and Ba were established in the mineral composition of the studied sediments. Maximum content of BaO (14.42 wt%) was detected in alkali K-feldspar in the clay sediments of modern alluvial complex (aQ_4). Crystallochemical formulas of different minerals were obtained.

Key words: Electron probe X-ray spectral microanalysis, mineral composition, Quaternary sediments, feldspars, ore minerals.

1. Introduction

Quaternary sediments were studied in the eastern part of the Tunkinsk's depression (the Southwestern Baikal region, the Republic of Buryatia) in the zone of erosion processes. In this territory gully processes are proceeding actively due to the prevalence of depth erosion. The loose cover represented by sediments of different geological-genetic complexes is most affected.

It should be noted that the research area is characterized by sharp continental climate. The period with negative average monthly temperatures of air lasts from October to April [1]. In the territory of the Tunkinsk's depression cryogenic processes (moisture migration, change of water phases, expansion and shrinkage of rocks during freezing and thawing) are developed [2].

Corresponding author: Shtel'makh Svetlana, researcher, research fields: X-ray fluorescence analysis of rocks, sediments and soils, geochemistry and mineralogy.

The work was supported by the Russian Foundation of Basic Research (project No. 05-05-97234).

2. Objects

The samples of the loess-like sediments were selected as objects of study located in several main areas within the Tunkinsk's depression.

The studied sediments are represented by lacustrine clayed sand (lQ_4), clay sediments of modern alluvial complex (aQ_4), as well as loess soils (loess-like sandy loams, loams) of deluvial-proluvial undifferentiated complex (dpQ), deluvial modern (dQ_4), and aeolian Upper Quaternary-modern (vQ_{3-4}) complexes.

The main areas were located in the district of the Zaktuy village in zone of the productive gulchs (observation point 1P on the map (Fig. 1)), in the gulch near the Elovka village (3P), in the soil-pit on the surface of a high floodplain of the Elovka river (4P), in the small gulchs on the left port side of the Elovka river within the original hillslope (7P), as well as in the small quarry in the area of young dormant volcanoes located a few kilometers from the Arshan settlement (12P) (Fig. 1). The studied samples were taken in the depth range from 0.7 to 2.4 m.

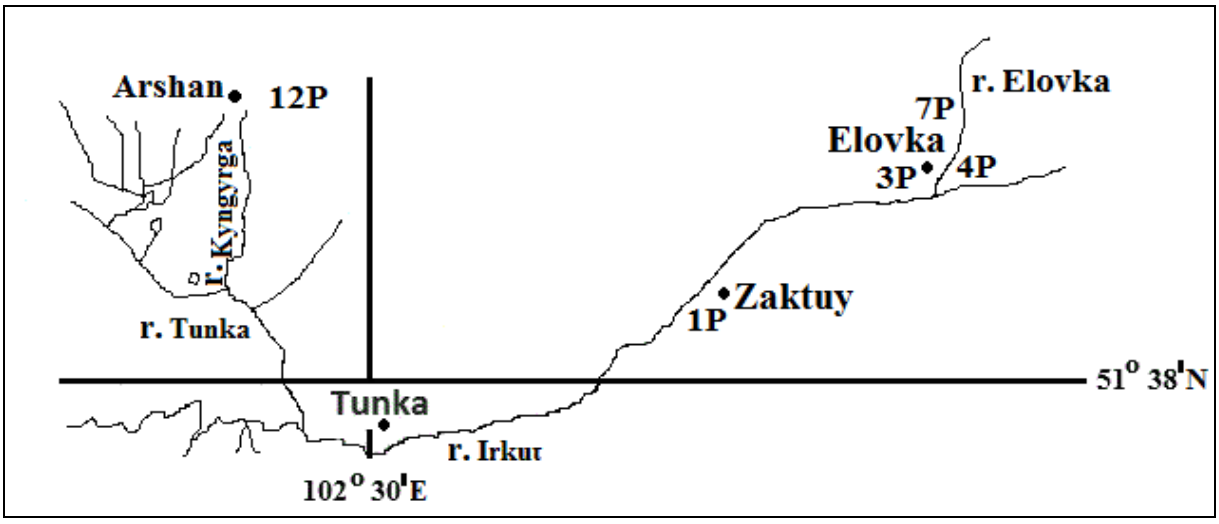

Fig. 1 Location map of subjects of research on the territory of the Tunkinsk's depression.

The rocks of metamorphic (biotite gneisses, marbles), intrusive (granosyenites) and effusive (basalts) geological formations, as well as conglomerates, sands and clays of the Pliocene are widespread in eastern part of the Tunkinsk's depression. These formations are the source of trace elements of the studied Quaternary sediments [3], and they have the significant effect on the mineral composition of these sediments.

3. Research Method

3.1 X-Ray Spectral Microanalysis (XRM)

All studies were performed using a microanalyzer JXA-8200 (JEOL Ltd., Japan) in Institute of Geochemistry named after A. P. Vinogradov (Irkutsk). This instrument is equipped with five wave spectrometers, an energy dispersive spectrometer with a SiLi detector (resolution of 133 eV for the line of Mn K_α), and detectors of secondary and backscattered electrons.

Wave spectrometers were used during the research. The accelerating voltage and the probe current intensity were 20 kV and 20 nA, respectively. The magnification was 100×.

The samples of the studied sediments were prepared as press-fit in epoxy resin and polished with diamond pastes to achieve a satisfactory surface required for analysis [4, 5].

The chemical composition was determined for 300 selected points. The concentrations of different chemical elements oxides were obtained. Also, maps of the chemical elements (Mg, Al, Si, K, Ca, Ti, Mn, Fe, and Ba) distribution were obtained. All images were made using backscattered electrons.

3.2 X-Ray Diffraction Analysis

X-ray diffraction analysis was carried out using a diffractometer DRON-3 (Russia) in Institute of the Earth's Crust (Irkutsk). The main parts of the diffractometer DRON-3 are an X-ray generator equipment, a goniometric unit, an automatic control unit, an electronic computing device, and an information output device [6].

The X-ray tube with a copper anode was used during the research. The electric potential difference and the electric current intensity of the X-ray tube are 25 kV and 20 mA, respectively. Also, the nickel filter was used.

The prepared suspensions from the samples of the studied sediments were deposited on glass for the study of the clay minerals. The air-dry samples and the samples saturated with ethylene glycol were used. Also, the samples calcined at 550 °C were used. The obtained X-ray powder diffraction patterns were

calculated and determined using special literature [7].

3.3 Calculation of Crystallochemical Formulas of Minerals

The PetroExplorer program developed by E. V. Korinevskiy (Institute of Mineralogy, Ural Branch of the Russian Academy of Sciences, Miass) [8] was used for calculation of the crystallochemical formulas of minerals in the samples of the studied sediments. The calculation of the crystallochemical formulas of ore minerals was carried out using the oxygen method [9].

4. Result and Discussions

4.1 General Features of the Mineral Composition

A large number of minerals, such as feldspars, micas, amphiboles, garnets, pyroxenes, ore minerals of titanium and iron, and zircons were detected in the microvolumes of the studied samples using X-ray spectral microanalysis.

It was found that feldspars of various chemical composition are most widely in the mineral composition of the studied sediments. Also, obtained maps of the chemical elements distribution showed the predominance of aluminosilicates in the mineral composition of the studied sediments. So, Al and Si were characterized by the greatest distribution among other elements (Mg, K, Ca, Ti, Mn, Fe, and Ba) where Mn and Ba were very dispersed.

Also, muscovite and biotite were identified among micas. Magnesian hornblende is the most prevalent compared to ferruginous hornblende and tschermakite among amphiboles. Garnets were represented mainly by the grossular ($Ca_3Al_2(SiO_4)_3$) and almandine ($Fe_3Al_2(SiO_4)_3$).

Diopside ($CaMg(Si_2O_6)$) predominates among pyroxenes in the mineral composition of the studied sediments. It is one of the main mineral species among monoclinic pyroxenes.

Ore minerals (ilmenite, titanomagnetite) were much less common in contrast to aluminosilicates.

Zircons were detected only in the sample of lacustrine clay sediments (lQ_4-gln) from gulch near the Elovka village from a depth of 1.3 m and in the sample of loess-like sandy loams (dpQ) (gulchs zone in the district of the Zaktuy village, depth 1.4 m) (observation points 1P and 3P).

Also, the rock-forming and the clay minerals were identified in the mineral composition of the studied sediments using X-ray diffraction analysis. In most cases, quartz, feldspar, and amphiboles were detected by this method among minerals related to the rock-forming.

Hydrous mica and chlorite prevailed over smectite and kaolinite among the clay minerals in the mineral composition of the studied loess-like sediments. This is due to the formation of the studied sediments in a relatively cold and arid climate [10]. As a result of cryogenic influences, the studied sediments are characterized by light particle size distribution, the presence of macropores. In some cases, the increase in the content of calcium carbonate is observed in sediments [11].

In addition to the rock-forming and the clay minerals, the mineral salts such as anhydrite (anhydrous gypsum) and gypsum, as well as calcium and magnesium carbonates (calcite and dolomite) were established by method of X-ray diffraction analysis. Possibly, the accumulation of mineral water-soluble salts such as gypsum was associated with the intense evaporation of groundwater from which dissolved salts precipitated. The maximum groundwater depth is in the range from 1 to 3 m at which salinization of the surface soil layers begins [12].

4.2 The Chemical Composition of Feldspars

Alkali feldspars and plagioclases were established in the studied sediments. Albite, oligoclase, andesine, and labrador were detected in plagioclases depending on the content of anorthite ($CaAl_2Si_2O_8$) (Fig. 2).

As can be seen in the mineral composition of the

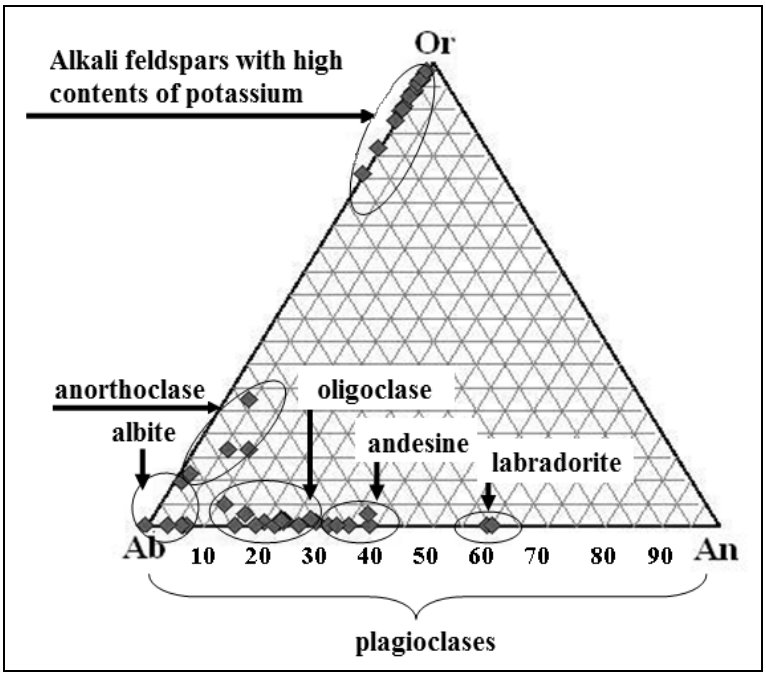

Fig. 2 Diagram of fluctuations in the chemical composition of feldspars [13].

studied sediments plagioclases prevail over alkali feldspars represented by anorthoclase and feldspars with high contents of potassium. The concentrations of Na_2O and K_2O vary in the ranges (in wt%): 6.620-9.784 and 1.927-4.558 in anorthoclases, respectively. Also, the contents of albite endmember vary from 68.31% to 86.53% in anorthoclases while the contents of anorthite and orthoclase endmembers change in the intervals (in %): 2.25-9.91 and 11.22-27.01, respectively.

In most cases, the concentrations of Na_2O do not exceed 1 wt% in alkali feldspars with high contents of potassium where the concentrations of K_2O are 15-16 wt% in contrast to plagioclases. The general formula for these alkali feldspars is ($KAlSi_3O_8$). The contents of orthoclases endmember vary from 75% to 98%. The concentrations of albite endmember change in the interval from 2.46% to 24.28%.

The common feature of the chemical composition of feldspars in the studied sediments is the presence of iron. The highest concentration (7.90 wt%) was established in anorthoclase (Fig. 3).

Oligoclase and albite are characterized by higher iron concentrations in contrast to alkali K-feldspars.

The distinctive feature of alkali feldspars chemical composition is the presence of barium (Table 1).

The concentrations of barium vary in a very wide range from 0.16 to 14.42 wt%. Maximum content of BaO (14.42 wt%) was detected in alkali K-feldspar in the sample of clay sediments of modern alluvial complex (aQ_4). This sample was selected in the soil-pit on the surface of a high floodplain of the Elovka river (observation point 4P).

You can see from the presented formulas of alkali K-feldspars that barium replaces potassium (Table 1). This is due to the similar sizes of atoms and ions of these elements. So, the radii of Ba and K atoms are 0.221 nm and 0.236 nm, respectively [14]. In the Linus Pauling system the radii of Ba^{2+} and K^{+} ions are 0.135 nm and 0.133 nm, respectively [15]. The aforecited values of ionic radii correspond to a coordination number (CN) that is 6.

As a result of calculations, it was found that iron is trivalent in the composition of all studied feldspars. In this case, isovalent isomorphism occurs between Fe^{3+} and Al^{3+} [16]. The radii of Fe^{3+} and Al^{3+} ions are 0.064 nm and 0.050 nm (CN is 6), respectively [15]. However, the difference in ionic radii of these cations

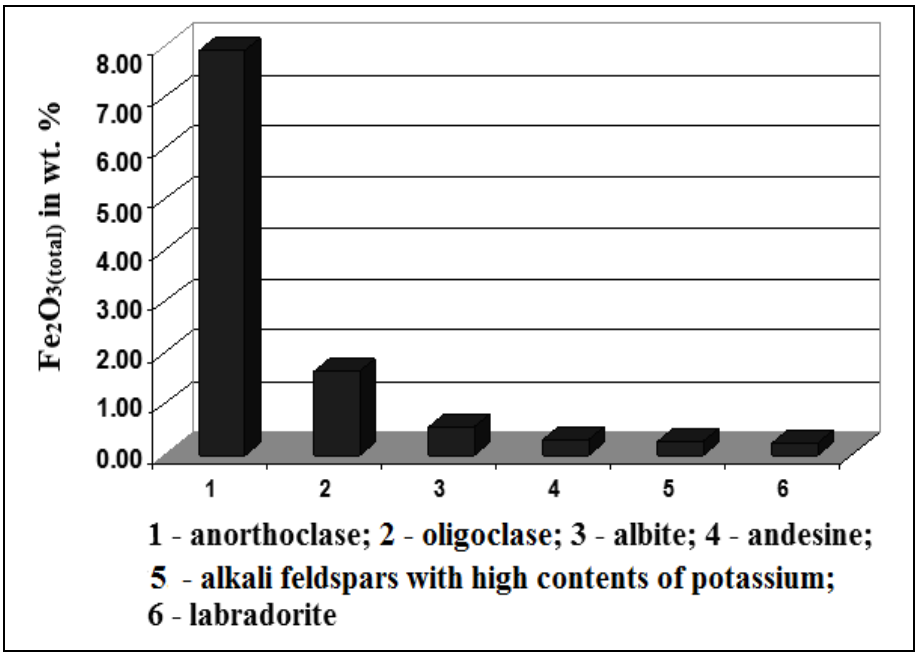

Fig. 3 Maximum iron concentrations in feldspars in the studied sediments.

Table 1 The chemical composition (wt%) of alkali feldspars in the studied sediments.

SiO_2	Na_2O	K_2O	Al_2O_3	$Fe_2O_{3(total)}$	BaO	∑	Crystallochemical formula
Loess-like sandy loams of deluvial-proluvial undifferentiated (dpQ) complex (observation point 1P)							
63.55	0.39	15.99	18.62	0.14	0.59	99.30	$(K_{0.954}Ba_{0.011}Na_{0.035})_{1.000}(Al_{1.026}Fe^{3+}_{0.002})_{1.028}Si_{2.972}O_8$
61.84	1.42	14.66	19.54	0.16	1.97	99.59	$(K_{0.872}Ba_{0.036}Na_{0.128})_{1.036}(Al_{1.075}Fe^{3+}_{0.003})_{1.078}Si_{2.886}O_8$
Clay sediments of modern alluvial (aQ4) complex (point 4P)							
50.37	0.74	9.40	21.80	0.26	14.42	97.00	$(K_{0.629}Ba_{0.297}Na_{0.075})_{1.001}(Al_{1.349}Fe^{3+}_{0.005})_{1.354}Si_{2.645}O_8$
64.20	0.44	16.49	18.80	0.18	0.16	100.27	$(K_{0.970}Ba_{0.003}Na_{0.039})_{1.012}(Al_{1.022}Fe^{3+}_{0.003})_{1.025}Si_{2.962}O_8$
Loess-like sandy loams of deluvial modern (dQ_4) complex (point 7P)							
62.63	0.53	15.85	19.16	0.21	1.27	99.66	$(K_{0.944}Ba_{0.023}Na_{0.048})_{1.015}(Al_{1.055}Fe^{3+}_{0.004})_{1.059}Si_{2.926}O_8$
64.32	2.71	12.86	19.77	0.21	0.95	100.82	$(K_{0.747}Ba_{0.017}Na_{0.240})_{1.004}(Al_{1.062}Fe^{3+}_{0.004})_{1.066}Si_{2.931}O_8$

is much larger as compared with the large ions of Ba and K.

4.3 The Chemical Composition of Micas

Muscovite and biotite were characterized by the greatest distribution among the minerals of micas group. Muscovite belongs to the group of aluminum micas while biotite is a magnesian-iron mica.

In most cases, the high contents of Al_2O_3 (36.68-37.24 wt%) were identified in the chemical composition of muscovite. The concentrations of K_2O vary from 11.09 to 13.12 wt% in muscovite. The contents of SiO_2 do not exceed 51 wt%. Also, in one case, relatively low concentration of sodium oxide (1.05 wt%) was detected in the chemical composition of muscovite from the sample of loess-like sandy loams of deluvial modern complex (dQ_4). This sample was selected in the gulch on the left port side of the Elovka river within the original hillslope (point 7P). The presence of sodium is associated with isomorphic substitution of K^+ ion by Na^+ ion [16]. In this case, the obtained muscovite formula is $K_{0.898}Na_{0.130}Al_{1.999}(Si_{3.213}Al_{0.787}O_{10})(OH)_2$.

The chemical composition of biotite is characterized by the high concentrations of iron and magnesium. The concentrations of $Fe_2O_{3(total)}$ vary from 18.34 to 37.19 wt%. The contents of MgO change from 8.47 to 14.14 wt%. The concentrations of

Al_2O_3 and SiO_2 do not exceed 21.11 and 40.87 wt%, respectively. The content of TiO_2 varies from 1.92 to 2.75 wt%.

In all cases, iron is divalent in biotite. Magnesium is divalent too. Magnesium and iron atoms are capable of replacing each other in any proportions, forming continuous solid solutions (phlogopite-biotite). In this case, entire isomorphism is observed between magnesium and iron wgich are in all studied biotites [17]. In tetrahedral layers Al^{3+} replaces Si^{4+} while Ti^{4+} ions replace tetrahedral Al^{3+} [17].

Fig. 4 shows REM images of biotite particles in the sample of lacustrine clay sediments (lQ_4-gln) from gulch near the Elovka village from a depth of 1.3 m (observation point 3P on the map (Fig. 1)).

The indicated numbers symbolize the points at which the chemical composition of biotite was determined. In the studied sample of lacustrine clay sediments in the chemical composition of biotite the concentrations of K_2O vary from 1.50 wt% (point 2 in Fig. 4) to 9.36 wt% (point 3 in Fig. 4). The content of K_2O is 5.01 wt% in point 1 (Fig. 4). Also, an increase in $Fe_2O_{3(total)}$ concentrations occurs with a decrease in K_2O contents. So, the chemical composition is characterized by the minimum concentration of K_2O (1.50 wt%) and the maximum content of $Fe_2O_{3(total)}$ (37.19 wt%) in the point 2 (Fig. 4) where obtained biotite formula is $K_{0.133}(Fe_{2.175}Mg_{0.955})_{3.13}(Si_{2.102}Al_{1.576}Ti_{0.113}O_{10})(OH)_2$.

A similar concentration reduction of K_2O is associated with the gradual conversion of biotite into hydrous mica (hydrobiotite). Crystal lattice instability of trioctahedral mica is associated with orientation of OH groups perpendicular to the plane of the layer. This leads to the convergence of hydrogen of hydroxyl groups with K^+ ion [18, 19].

4.4 The Chemical Composition of Amphiboles

Calcium amphiboles are the most common in the studied sediments. Fig. 5 shows that magnesian hornblende is the most prevalent compared to tschermakite and ferrotschermakite.

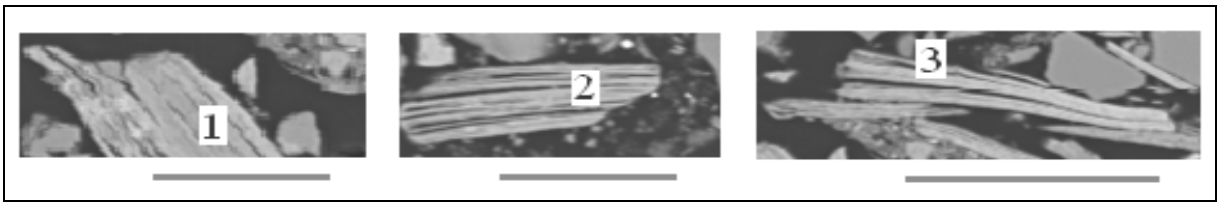

Fig. 4 REM images of biotite particles in the sample of lacustrine clay sediments (lQ_4-gln). The length of the scale rule is 0.1 mm.

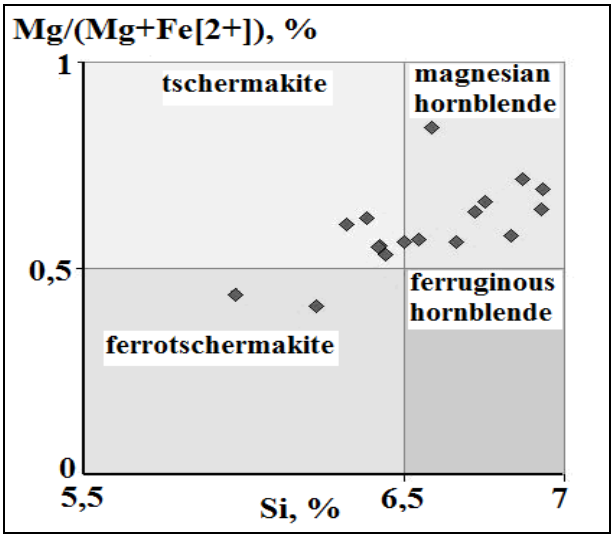

Fig. 5 Binary chart of the IMA for classification of calcium amphiboles [20].

Also, actinolite and hastingsite were identified among calcium amphiboles. Actinolite is characterized by the low concentrations of Al_2O_3 and Na_2O compared to magnesian hornblende. The minimum contents of aluminum and sodium oxides are 2.52 and 0.27 wt% in actinolite, respectively. Hastingsite is characterized by the higher concentrations of TiO_2 (more 3 wt%) and $Fe_2O_{3(total)}$ (more 22 wt%) compared to magnesian hornblende and actinolite in which the contents of titanium and iron oxides do not exceed 0.6 and 15 wt%, respectively.

The chemical composition of magnesian hornblende is characterized by rather high contents of Cr_2O_3 which vary from 0.13 to 0.74 wt%. In addition, the concentrations of Cr_2O_3 increase with increasing of Al_2O_3 contents. It is established that Cr^{3+} replaces Al^{vi} in magnesian hornblende and actinolite. Also, ions of Fe^{2+}, Fe^{3+} and Mn^{2+} replace Mg^{2+} in magnesian hornblende and hastingsite. The chemical composition of hastingsite is characterized by small contents (less than 0.20 wt%) ZrO_2. Zr^{4+} ions replace Ti^{4+} ions in hastingsite (Table 2).

It should be noted that Al^{iv} prevails over Al^{vi} in the chemical composition of amphiboles. Also, this can be seen from the obtained crystallochemical formulas which were presented in Table 2. The content of Al^{vi} in amphiboles is primarily controlled by rock chemical composition and pressure, with high pressure favouring high Al^{vi} [21]. The maximum content of Al^{vi} will occur in amphiboles crystallized in highly aluminous environments with moderate or low contents of alkaline elements and under high pressures [21]. Relative increase of Al^{vi} content in amphibole is associated with an increase of pressure during mineral formation [22, 23]. In most cases, the total contents of K_2O and Na_2O vary from 1.52 to 3.92 wt. % in calcium amphiboles in the studied sediments samples. Although, the total contents of this alkaline elements do not exceed 1.10 wt% in actinolites. Also, you can see a slight difference in contents of Al^{vi} and Al^{iv} as well as the complete absence of ferric iron in the obtained crystallochemical formula of one from the actinolites (Table 2). In some cases, the complete absence of Al^{vi} was found in actinolites in which there was no K_2O and ferric iron too, and the concentration of Na_2O was about 1.0 wt%. These actinolites were identified in the mineral composition of the sample of lacustrine clay sediments (lQ_4-gln) from gulch near the village Elovka from a depth of 1.3 m (point 3P). The similar distribution of Al^{vi} and Al^{iv} can be associated with low concentrations of Al_2O_3 in the chemical composition of the studied actinolites.

Based on the aforecited facts, we assume that the formation of the studied amphiboles occurred under low pressures.

Table 2 The chemical composition (wt%) of calcium amphiboles in samples of the studied sediments.

SiO_2	Al_2O_3	Cr_2O_3	K_2O	Na_2O	TiO_2	ZrO_2	CaO	MgO	MnO	$Fe_2O_{3(total)}$	∑
Magnesian hornblende in the sample of loess-like sandy loams of deluvial modern complex (dQ_4) (point 7P)											
46.14	11.16	0.74	0.18	2.03	0.55	-	11.25	15.92	0.13	9.30	97.40
$(Na_{0.405}K_{0.033})_{0.438}(Na_{0.155}Ca_{1.720}Fe^{2+}_{0.108}Mn_{0.016})_{1.999}(Mg_{3.387}Fe^{3+}_{0.455}Fe^{2+}_{0.546}Ti_{0.059}Al^{vi}_{0.469}Cr_{0.084})_{5.000}(Si_{6.590}Al^{iv}_{1.410})_{8.000}O_{22}(OH)_2$											
Actinolite in the sample of loess-like sandy loams of deluvial-proluvial undifferentiated (dpQ) complex (point 1P)											
53.99	2.52	0.11	0.20	0.27	0.14	-	13.72	14.39	-	13.67	99.00
$(Na_{0.075}K_{0.037})_{0.112}Ca_{2.114}(Mg_{3.084}Fe^{2+}_{1.642}Ti_{0.015}Al^{vi}_{0.195}Cr_{0,011})_{4.947}(Si_{7.767}Al^{iv}_{0.233})_{8.000}O_{22}(OH)_2$											
Hastingsite in the sample of loess-like sandy loams of aeolian Upper Quaternary - modern ($vQ_{3\text{-}4}$) complex (point 12P)											
40.83	10.30	-	1.20	2.72	3.48	0.16	10.03	7.16	0.58	22.48	98.94
$(Na_{0.492}K_{0.233})_{0.725}(Na_{0.311}Ca_{1.639}Mn_{0.050})_{2.000}(Mg_{1.628}Mn_{0.025}Fe^{3+}_{0.472}Fe^{2+}_{2.392}Ti_{0.400}Zr_{0.017}Al^{vi}_{0.084})_{5.018}(Si_{6.231}Al^{iv}_{1.769})_{8.000}O_{22}(OH)_2$											
Tschermakite in the sample of clay sediments of modern alluvial (aQ_4) complex (point 4P)											
43.71	12.64	-	1.21	1.06	0.69	-	11.97	9.50	0.37	17.88	99.03
$(Na_{0.244}K_{0.227})_{0.471}(Na_{0.058}Ca_{1.891}Mn_{0.046}Fe^{2+}_{0.005})_{2.000}(Mg_{2.086}Fe^{3+}_{0.348}Fe^{2+}_{1.853}Ti_{0.076}Al^{vi}_{0.642})_{5.005}(Si_{6.445}Al^{iv}_{1.555})_{8.000}O_{22}(OH)_2$											

The symbol "-" means that the component is not detected in the chemical composition of amphiboles.

4.5 The Chemical Composition of Ore Minerals of Titanium and Iron

Ilmenite ($FeTiO_3$) and titanomagnetite (Fe_2TiO_4) were identified both in the form of individual grains and inclusions in various aluminosilicates in the mineral composition of the studied sediments. The average concentrations of iron and titanium oxides are 46.75 and 50.38 wt% in ilmenite, respectively. Titanomagnetite is characterized by a higher average concentration of iron oxides which increases to 66.13 wt% while the average concentration of TiO_2 decreases to 28.31 wt% in contrast to ilmenite. The contents of MgO change from 0.14 to 2.70 wt% in ilmenite. The concentrations of MnO vary from 0.50 to 1.29 wt% in $FeTiO_3$. The contents of MgO do not exceed 1.90 wt% in titanomagnetite. The concentrations of MnO vary in a narrow range from 0.41 to 0.80 wt% in Fe_2TiO_4. In all cases, iron is divalent in ilmenite. However, ferrous iron and ferric iron were identified in the composition of titanomagnetite. Ferrous iron prevails over ferric iron in titanomagnetite. Ions of Fe^{2+} are isomorphically replaced by ions of Mg^{2+} and Mn^{2+} in both ilmenite and titanomagnetite [24, 25]. Also, SiO_2 and Al_2O_3 are identified in the composition of these minerals when they are inclusions in aluminosilicates. In most cases, total contents of these oxides do not exceed 1.0 wt%. Also, the oxides of chalcophilic elements (Cu and Zn) as well as ZrO_2 were detected in the chemical composition of ilmenites. Total concentrations of CuO and ZnO do not exceed 1.0 wt% in ilmenites too while the contents of ZrO_2 vary in a fairly narrow range from 0.18 to 0.26 wt%. In ilmenite of the sample of loess-like sandy loams of aeolian Upper Quaternary-modern ($vQ_{3\text{-}4}$) complex from the small quarry in the area of young dormant volcanoes (point 12P) the content of MnO and total concentration of CuO and ZnO are 1.19 and 0.89 wt%, respectively. The content of Al_2O_3 are 0.29 wt% in this ilmenite. In this case, the obtained crystallochemical formula is $(Fe_{0.983}Mn_{0.026}Cu_{0.012}Zn_{0.005})_{1.026}(Ti_{0.981}Al_{0,009})_{0,990}O_3$.

You can see that Cu^{2+} and Zn^{2+} ions are associated with Mn^{2+} ions. Al^{3+} ions replace Ti^{4+} ions. Also, Si^{4+} and Zr^{4+} ions replace Ti^{4+} ions in ilmenites containing SiO_2 and ZrO_2.

Total concentrations of CuO and ZnO do not exceed 0.50 wt% in titanomagnetite. The contents of Cr_2O_3 and ZrO_2 are less than 0.25 wt% in this mineral. The maximum number of impurity elements (Al, Si, Mg, Mn, Cr, Cu, Zn, and Zr) was detected in the chemical composition of titanomagnetite in the sample of loess-like sandy loams of deluvial-proluvial undifferentiated (dpQ) complex from zone of the productive gulchs in the district of the Zaktuy village (point 1P). In this case, the obtained crystallochemical formula of tita-nomagnetite is characterized by significant differences from the theoretical formula (Fe_2TiO_4). The obtained formula is $(Fe^{2+}_{1.685}Mg_{0.080}Mn_{0.012}Cu_{0.008}Zn_{0.004})_{1.789}$ $(Ti_{0.849}Zr_{0.002}Si_{0.034}Fe^{3+}_{0.246}Al_{0.031}Cr_{0.006})_{1.168}O_4$.

Cr^{3+} ions replace Al^{3+} ions while Al^{3+} ions replace Fe^{3+} ions in chemical composition of this titanomagnetite. Isomorphous substitutions were identified between Al^{3+} and Fe^{3+} ions in alkali K-feldspars too.

It should be noted that ilmenite and titanomagnetite are characterized by a large number of impurity elements in the mineral composition of the studied loess-like sediments.

5. Conclusions

As a result of the study, some general features of the mineral composition of the studied loess-like sediments were established. It was found with the help of X-ray diffraction analysis that hydromica and chlorite prevailed over smectite and kaolinite among the clay minerals in the mineral composition of the studied loess-like sediments. Also, it was found with the help of X-ray spectral microanalysis that the gradual conversion of biotite into hydrous mica (hydrobiotite) occurs. The prevalence of hydrous mica

and chlorite is associated with the formation of the studied loess-like sediments in a relatively cold arid climate.

The localization centers of Cr, Cu, Zn, Zr, and Ba were established in the mineral composition of the studied sediments. It was established that feldspars enriched with potassium are the main localization center of Ba while Cu and Zn accumulate only in ore minerals. Cr accumulates both in amphiboles and titanomagnetite. Zr accumulates only in hastingsite and ore minerals. The concentrations of Cr_2O_3 increase with increasing of Al_2O_3 content. A similar relationship was found between the concentrations of ZrO_2 and TiO_2.

The detailed analysis of calcium amphiboles and the study of the distribution of Al^{vi} and A^{iv} in them suggest the formation of these minerals under low pressures.

Also, calcium garnets (grossular) distributed widely in the mineral composition of the studied sediments were formed under lower pressure in contrast to pyrope, almandine and spessartine.

Acknowledgments

Authors thank the candidates of geological and mineralogical sciences L. Z. Reznitskiy and V. B. Savel'yeva as well as Mitichkin M. A. for help in the investigation of minerals. Also, authors gratefully acknowledge T. S. Fileva for assistance in the performance of the investigations.

This study was performed using equipments located at the Center for Geodynamics and Geochronology and the Center for Isotope-geochemical research (Institute of the Earth's Crust, SB RAS, and Institute of Geochemistry named after A. P. Vinogradov, SB RAS, Irkutsk, Russia).

References

[1] Koshinskiy, S. D., and Drobyshev, A. D. 1975. "Irkutsk Region and the Southwestern Part of the Buryat Autonomous Soviet Socialist Republic. Part 2: Atmospheric Precipitation." In *Handbook of the Climate of the USSR. Meteorological Data for Individual Years.* Vol. 22. Irkutsk: Publishing House of the Irkutsk Hydrometeorological Service. (in Russian)

[2] Leshchikov, F. N. 1978. *Frozen Rocks of the Angara Region and the Baikal Region*. Novosibirsk: Publishing House "Nauka". (in Russian)

[3] Ryashchenko, T. G., and Shtel'makh, S. I. 2008. "Microelements in Dispersive Soils of Different Geological-Genetic Complexes (on the Example of Main Areas in the Tunkinsk's Depression)." *Geology, Prospecting and Exploration of Ore Deposits* 6 (32): 161-8. (in Russian)

[4] Pavlova, L. A. 2014. *Electron Probe X-Ray Spectral Microanalysis and Its Application*. Saarbrucken, Deutschland: International Publishing House, LAP Lambert Academic Publishing. (in Russian)

[5] Pavlova, L. A. 2011. "Dependence of Determination Quality on Performance Capacity of Researching Technique, Exemplified by the Electron Probe X-Ray Microanalysis." In *Modern Approaches to Quality Control*, edited by Ahmed Badr Eldin et al. Intech Open Access Publisher.

[6] Umanskiy, Y. S., Skakov, Y. A., Ivanov, A. N., and Rastorguev, L. N. 1982. *Crystallography, Radiography and Electron Microscopy*. Moscow: Publishing House "Metallurgy". (in Russian)

[7] Frank-Kamenetskiy, V. A. 1983. *X-Ray Diffraction of the Main Types of Rock-Forming Minerals*. Leningrad: Publishing House "Nedra". (in Russian)

[8] Korinevskiy, E. V. 2009. "Petrochemical Features of the Quartzite-Shale Strata of the Ilmenogorsk Metamorphic Complex." *Ural Mineralogical Collection* 16: 74-85. (in Russian)

[9] Urusov, V. S. 1987. *Theoretical Crystal Chemistry*. Moscow: Publishing House of Moscow State University. (in Russian)

[10] Rusanov, G. G. 2009. "About Pliocene Cooling of the Climate in the Northeastern Foothills of Altai." *Successes in Modern Natural Sciences* 6: 56-9. (in Russian)

[11] Ryashchenko, T. G., Akulova, V. V., and Rubtsova, M. N. 2014. "The Processes of Aeolian Sedimentation in the Baikal Region." *Bulletin of ISTU* 93 (10): 109-14. (in Russian)

[12] Savich, V. I., Sedykh, V. A., and Geraskin, M. M. 2016. *Soil Protection*. Moscow: Publishin House "Prospect". (in Russian)

[13] Deer, W. A., Howie, R. A., and Zusman, L. 1966. *Rock-Forming Minerals*, edited by Yakovenko, M. E. Moscow: Publishin House "Mir". (in Russian)

[14] Pauling, L., and Pauling, P. 1978. *Chemistry*, edited by Karapetyants, M. L. Moscow: Publishin House "Mir". (in Russian)

[15] Pauling, L. 1960. *The Nature of the Chemical Bond*, 3rd ed. Ithaca, NY: Cornell University Press.

[16] Urusov, V. S. 1977. *Theory of Isomorphic Miscibility*. Moscow: Publishin House "Nauka". (in Russian)

[17] Ripp, G. S., Doroshkevich, A. G., Karmanov, N. S., and Kanakin, S. V. 2009. "Mica of the Khalyutinskiy Carbonatite Deposit (Western Transbaikalia)." *Notes of the Russian Mineralogical Society* 138 (1): 108-23. (in Russian)

[18] Sokolova, T. A., Tolpeshta, I. I., and Topunova, I. V. 2010. "Weathering of Biotite in Podzolic Soil under Conditions of Model Field Experiment." *Soil Science* 10: 1239-48. (in Russian)

[19] Basset, W. A. 1960. "Role of Hydroxyl Orientation in Mica Alteration." *Bull. Geol. Soc. Am.* 71 (4): 449-56.

[20] Leake, B. E., Woolley, A. R., Arps, C. E. S., et al. 1997. "Nomenclature of Amphiboles: Report of the Subcommittee on Amphiboles of the International Mineralogical Association Commission on New Minerals and Mineral Names." *Eur. J. Mineral* 9 (3): 623-51.

[21] Leake, B. E. 1971. "On Aluminous and Edenitic Horblendes." *Mineral* 38 (296): 389-407.

[22] Raase, P. 1974. "Al and Ti Content of Hornblende, Indicators of Pressure and Temperature of Regional Metamorphism." *Contrib. to Mineral. and Petrol* 45 (3): 231-6.

[23] Brown, E. H. 1977. "The Crossite Content of Ca-Amphibole as a Guide to Pressure of Metamorphism." *J. Petrol* 18 (1): 53-72.

[24] Neumann, E. R. 1974. "The Distribution of Mn^{2+} and Fe^{2+} between Ilmenites and Magnetites in Igneous Rocks." *American Journal of Science* 274: 1074-88.

[25] Zhou, M. F., Robinson, P. T., Lesher, C. M., Keays, R. R., Zhang, C. J., and Malpas, J. 2005. "Geochemistry, Petrogenesis and Metallogenesis of the Panzhihua Gabbroic Layered Intrusion and Associated Fe-Ti-V Oxide Deposits, Sichuan Province, SW China." *J. of Petrology* 46 (11): 2253-80.